**Atmospheric
Chemistry
and Physics
Discussions**

Airborne lidar measurements of surface ozone depletion over Arctic sea ice

J. A. Seabrook[1], **J. A. Whiteway**[1], **L. H. Gray**[1], **R. Staebler**[2], **and A. Herber**[3]

[1]Centre for Research in Earth and Space Science (CRESS), York University, 4700 Keele Street, Toronto, Ontario, M3J 1P3, Canada
[2]Environment Canada, 4905 Dufferin Street, Toronto, Ontario, M3H 5T4, Canada
[3]Alfred Wegener Institute, Bussestrasse 24, 27570 Bremerhaven, Germany

Correspondence to: J. Whiteway (whiteway@yorku.ca)

ACPD

13, 1435–1453, 2013

Airborne lidar measurements of surface ozone depletion

J. A. Seabrook et al.

Title Page

Abstract	Introduction
Conclusions	References
Tables	Figures

◄◄ | ►►
◄ | ►

Back | Close

Full Screen / Esc

Printer-friendly Version

Interactive Discussion

Abstract

A differential absorption lidar (DIAL) for measurement of atmospheric ozone concentration was operated aboard the Polar-5 research aircraft in order to study ozone depletions over Arctic sea ice. The lidar measurements during a flight over the sea ice north of Barrow, Alaska on 3 April 2011 found a surface level depletion of ozone over a range of 300 km. The photochemical destruction of ground level ozone was strongest at the most northern point of the flight, and steadily decreased towards land. All the observed ozone depleted air throughout the flight occurred within 300 m of the sea ice surface. A back-trajectory analysis of the air measured throughout the flight indicated that the ozone depleted air originated from the north over the ice. Air at the surface that was not depleted in ozone had originated from over land to the south. An investigation into the altitude history of the ozone depleted air suggests a strong inverse correlation between measured ozone levels up to 1700 m in altitude, and the amount of time the air directly interacted with the sea ice.

1 Introduction

It has been established that ozone becomes depleted in air near the sea ice surface during the polar sunrise period in the Arctic (Oltmans, 1981; Oltmans and Komhyr, 1986; Bottenheim et al., 1986; Barrie et al., 1989; Seabrook et al., 2011) as well as the Antarctic (Jones el al., 2010). The observations find episodes when the ozone-mixing ratio at the surface decreases from normal (30–40 ppbv) levels to near zero for periods ranging from hours to weeks at a time. The currently accepted mechanism for the destruction of tropospheric ozone involves the release of Bromine salt ions from fresh sea ice. Photochemical reactions convert the inert Bromine into reactive Br atoms that deplete ozone in the boundary layer in a catalytic reaction cycle (Ridley et al., 2003). This is consistent with the coincident detection of greater concentrations of BrO during ozone depletion events (Barrie et al., 1989; McConnell et al., 1992). The

frequency and strength of these ozone depletions has implications for the overall mercury contamination of the snow/snowpack as the photochemical oxidation of gaseous elemental mercury (GEM) into total particulate mercury (TPM) and reactive gaseous mercury (RGM) is strongly correlated to ozone depletion events and the presence of reactive bromine (Lu et al., 2001; Steffen et al., 2008). There have been measurements that were interpreted as indicating that that ODEs can occur in air above the surface layer that is not directly in contact with the sea ice surface (e.g. McElroy et al., 1999), and one of aims of the study reported here was to determine whether there was evidence for this.

In order to investigate spatial structure of Arctic surface ozone depletion events, a differential absorption, light detection and ranging instrument (Differential Absorption LIDAR or DIAL) for the measurement of tropospheric ozone was installed on-board the Polar-5 research aircraft (Basler BT-67: rebuilt and modernized DC-3) as part of the PAMARCMIP 2011 (Pan-Arctic Measurements and Arctic Regional climate model simulations) measurement campaign (Herber et al., 2012). Several flights out over the frozen Arctic Ocean, with the ozone DIAL mounted aboard the aircraft for downward viewing, were carried out from Barrow, Alaska, during April 2011. The observed structure of the surface ozone depletion events along the flight track provided a unique view that has been applied to assess the conditions in which the ozone depletion events occur.

2 Measurement technique

The basic DIAL method is to emit pulses of light into the atmosphere and record the backscatter signal as a function of time, or equivalently range. For a UV wavelength absorbed significantly only by ozone, the backscatter signal is described as

$$P(R,\lambda) = \frac{C}{R^2}\beta(R,\lambda)\exp\left[-2\int_0^R [\sigma(\lambda)\,n(R) + \alpha(R,\lambda)]\,\mathrm{d}R\right] \qquad (1)$$

where $P(R,\lambda)$ is the instantaneous received power from range R. The backscatter coefficient, $\beta(R,\lambda)$, represents the fraction of light scattered backward per unit length and per unit solid angle. The extinction coefficient, $\alpha(R,\lambda)$, is the fractional decrease in laser pulse intensity per unit length due to scattering. The product of the ozone number density and absorption cross section, $\sigma(\lambda)\,n(R)$, is the fractional decrease in laser pulse energy per unit length due to absorption by ozone molecules. C is a system constant that takes into account characteristics such as transmitted laser pulse energy, receiver aperture area, system optical throughput, and detector efficiency.

The lidar emits multiple wavelengths in the UV that lie on the broad Hartley ozone absorption band. The differential absorption between wavelengths with different absorption cross sections is employed to derive the ozone density. Ozone retrieval from the recorded signal is performed by calculating the slope of the logarithmic ratio of any pair of these signals as

$$n(R) = \frac{-1}{2(\sigma(\lambda_{\mathrm{on}}) - \sigma(\lambda_{\mathrm{off}}))}\left\{\frac{\mathrm{d}}{\mathrm{d}R}\left[\ln\left(\frac{P_{\mathrm{on}}(R)}{P_{\mathrm{off}}(R)}\right)\right] + 2(\alpha_{\mathrm{m}}(R,\lambda_{\mathrm{on}}) - \alpha_{\mathrm{m}}(R,\lambda_{\mathrm{off}}))\right\} \qquad (2)$$

where "on" denotes the wavelength with the larger ozone absorption cross section, and the term $2(\alpha_{\mathrm{m}}(R,\lambda_{\mathrm{on}}) - \alpha_{\mathrm{m}}(R,\lambda_{\mathrm{off}}))$ is a correction factor to account for differential extinction due to molecular scattering. Ozone was derived using the temperature dependent ozone absorption cross-sections from the HITRAN 2008 database (Rothman et al., 2009)

For the measurements in this study there was not a significant contribution to the signal by aerosol and cloud particles, and the differential absorption and scattering due to aerosol had a negligible effect on the derived ozone concentration. Measurements

where clouds were a significant factor were omitted when performing the analysis. The molecular scattering and extinction coefficients were calculated from atmospheric densities determined using data from meteorological radiosondes launched from Barrow AK MET station (71.30° N, 156.78° W).

A schematic diagram of the DIAL system is shown in Fig. 1. The fourth harmonic of a Q-switched Nd:YAG laser (266 nm, 70 mJ per pulse, 20 Hz repetition rate) is focused into the center of a cell filled with 140 PSI of CO_2 where stimulated Raman scattering into the first to third Stokes lines generates light with wavelengths of 276 nm, 287 nm and 299 nm (Nakazato et al., 2007). The diameter of the multi-wavelength output beam was expanded by a factor of three to reduce the divergence to about 0.2 mrad before it was directed into the atmosphere. Full overlap between the emitted laser pulse and the telescope field of view occurred at a range of 500 m and the signal received from within that range was not used in the ozone analysis.

Backscattered light was collected with a 15 cm off-axis parabolic mirror and a 1.5 mm diameter fused-end optical fiber bundle positioned in the focal plane, 500 mm from the mirror, to form a receiver field of view of 3 mrad. The four wavelengths were separated in the receiver by the transmittance and reflectance from a series of tilted interference filters with bandwidths of 1 nm. Photomultipliers were used to detect the optical signals and the data acquisition employed both analog to digital conversion and photon counting in order to achieve linearity over a high dynamic range. The raw data was recorded with a range gate of 7.5 m and an integration period of 200 laser shots (10 s). The collected LIDAR profiles were averaged spatially and temporally in order to reduce the measurement uncertainty. The 266/287 nm analog signals were used to generate ozone profiles to a range of 2 km. At greater ranges, photon-counting signals were used to determine ozone levels near the ground.

The DIAL was installed within a single aircraft rack (56 × 64 × 130 cm), that is a self-contained unit (apart from the laser power supply) with internal thermal control and vibration isolation. The laser and telescope view out through a window on the rack which consists of two optical quality, UV anti-reflection coated glass plates, with Argon

Title Page

Abstract	Introduction
Conclusions	References
Tables	Figures

◄ | ►

◄ | ►

Back | Close

Full Screen / Esc

Printer-friendly Version

Interactive Discussion

gas filling the gap in order to avoid frosting. The rack is mounted to the seat rails with the window aligned above a port that is open to the atmosphere below the aircraft.

3 Measurements

On 2 April 2011, at 22:00 UTC, the Polar 5 departed Barrow for a flight track over the sea ice for a distance of 325 km to the north east. The first half of the flight, shown in black in Fig. 2, was a low level flight 100–200 m above the sea ice. The DIAL measurements were carried out only during the return flight leg (red in Fig. 2) while the aircraft was at a height of 2.2 km. A contour plot of the DIAL ozone measurements along this flight track is shown in Fig. 3. The lidar return signals used in this contour were averaged temporally over a window of 200 s, which corresponds to an average distance of approximately 12 km at the aircraft mean ground speed of 220 km hr^{-1}. Spatial averaging was also applied to the recorded signals such that the vertical resolution was 22.5 m for the analog and 75 m for the photon counting.

A persistent depletion of ozone was observed close to the surface throughout the flight. At the beginning of the measurement (case A), approximately 300 km northeast of the nearest land mass, ozone levels of 10 ppbv were observed at the surface, extending up to an altitude of 250 m above the sea ice. Above 250 m the mixing ratio increased until at an altitude of 400 m, background levels of approximately 40 ppbv were observed. The general trend throughout this flight is that depleted ozone concentration increased toward land while the vertical depth depletion also decreased. Within 20 km of the coast the depletion is almost non-existent.

In-situ ozone measurements were taken using a TE49C (Thermo Electron Inc., USA) with an air-sampling inlet located at the top of the aircraft. This provided a validation for the DIAL ozone measurements near the ice surface. The aircraft height on the outbound flight path was mostly within 100 m of the surface for sea ice thickness measurements, but at five locations there were ascents to heights ranging from 150–200 m for instrument calibrations followed by immediate descent (Fig. 4). These ascents provided

vertical profiles of in situ ozone measurements that can be compared with the DIAL measurements on the return flight leg. Figure 5 shows the ozone vertical profiles measured with the DIAL at three locations that will be used for case studies in the analysis. The location for the vertical profile of ozone measured by the DIAL in case-B (Fig. 5b) corresponds to the position of an in situ vertical profile taken during the outbound portion of the flight (the position is labeled as case B1 in Fig. 4b) as determined by a backwards trajectory calculation (shown as blue in Fig. 2) of the air from the point of the in situ measurement during the vertical ascent/descent of the aircraft. The DIAL and in situ vertical profile measurements are seen to be in agreement within the TECO accuracy of ± 1 ppb, and the DIAL measurement uncertainty of ± 3.5 ppb at 150 m above the surface of the ice.

4 Analysis

A back trajectory analysis of the air measured by the DIAL during the flight was performed. This analysis made use of the NOAA HYSPLIT model (Draxler and Hess, 1998), using GDAS (Global Data Assimilation System) meteorological data. The historical back-trajectories were calculated every two minutes for the period of time in which the DIAL was active for heights ranging from 100 m to 2000 m above sea level and were calculated for a 6-day period backward starting from the GPS location of the aircraft at each time interval.

The period of time in which the strongest depletion was observed (case-A), occurred at the Northern most track of the flight, approximately 300 km from the northern tip of Alaska (indicated as case-A in Fig. 3). The ozone-mixing ratio was less than 10 ppbv up to a height of 250 m and then increased to the background level of 30–40 ppbv at height 400 m. In this case the back trajectories shown in Fig. 6a indicate that the air up to a height of 1000 m originated from the East over the arctic sea ice. An analysis of the altitude history for case-A (Fig. 7a) indicates that the air at 100 m and 300 m above the ice surface had spent significant time below 350 m in the previous days, while the

back trajectories starting at heights 500 m and 1000 m did not spend any time below 350 m in the previous six days.

In case-B, approximately 140 km from land, the ozone depletion was observed to extend from the surface to a height of about 200 m (Figs. 3 and 5b). The depleted ozone concentration was not as low as observed in case-A (Figs. 3 and 5a). Back trajectory analysis (Fig. 6b) indicates that the origin of the measured air at an altitude of 100 m had shifted slightly to the south, such that the air closest to the ground spent much more time over land than over the sea ice in comparison to case-A. The altitude history (Fig. 7b) shows that air measured at height 300 m spent much less time below an altitude of 350 m in comparison to case-A.

Near the end of the flight (case-C), as the aircraft approached the coastline, the DIAL measured normal background levels of ozone (Figs. 3 and 5c). There was no ozone depletion event at the coastline. Back-trajectory analysis indicates that the air at 100 m a.s.l., while spending the previous 60 h within the stable boundary layer, originated from the south and was not in contact with sea ice over the Arctic Ocean (Fig. 6c). The air measured at 300 m a.s.l. spent very little time within 300 m of the sea ice prior to being measured, and the air above 300 m spent no time within 300 m of the sea ice during the six days prior to being measured near Barrow, AK (Fig. 7c).

This case study indicates that there is a correspondence between the ozone concentrations over the sea ice, and the history of the air. By calculating the amount of time a back-trajectory spent within 350 m of the sea ice over the previous few days, and comparing that with the measured ozone value, it was found that lower ozone mixing ratios were associated with air that had spent a longer amount of time in close proximity with the sea ice (Fig. 8). The general trend was that longer periods of time near the sea ice were associated with lower measured ozone mixing ratios.

5   Conclusions

The airborne DIAL measurements provided a continuous record of the vertical structure of a surface ozone depletion event over a horizontal range of 300 km. At a distance of 300 km from the Alaska coastline the layer of air adjacent to the sea ice was depleted in ozone up to a height of 300–400 m above the surface. Backward trajectory analysis indicated that the ozone-depleted air had spent extended periods of time within 350 m of sea ice. Close to the coastline the air was not depleted in ozone, and the corresponding back-trajectory indicated that this air had spent significant time over land, or did not have a history of being within the surface layer over the sea ice.

One of the aims of the experiment was to determine whether or not there was evidence for ozone depletion in air that was not adjacent to the sea ice surface, as suggested by McElroy et al. (1999). No such evidence was found during the flight reported here, or in two other flights with the DIAL installed on the Polar-5 aircraft. The results indicate that the ozone depletions occurred only in air that had been in contact with the ice surface. All of the air that was measured to be depleted in ozone was found to have a recent history of being confined to within 300 m of the surface. There were no observations of ozone-depleted air that was not connected to the surface. This is consistent with the findings of a previous study in which the same DIAL instrument provided measurements of ozone from the surface on board the Amundsen Coast Guard Icebreaker ship (Seabrook et al., 2011). The result is also consistent with previous studies using back-trajectory analysis (Bottenheim et al., 2009; Frieß et al., 2004) that have found a correlation between Arctic ozone depletion events and the length of time prior to being sampled that an air mass was within the surface layer over the sea ice.

References

Barrie, L., Hartog, G., Bottenheim, J., and Landsberger, S.: Anthropogenic aerosols and gases in the lower troposphere at Alert Canada in April 1986, J. Atmos. Chem., 9, 101–127, 1989.

Bottenheim, J., Gallant, A., and Brice, K.: Measurements of NO_y species and O_3 at 82° N latitude, Geophys. Res. Lett., 13, 113–116, 1986.

Bottenheim, J. W., Netcheva, S., Morin, S., and Nghiem, S. V.: Ozone in the boundary layer air over the Arctic Ocean: measurements during the TARA transpolar drift 2006–2008, Atmos. Chem. Phys., 9, 4545–4557, doi:10.5194/acp-9-4545-2009, 2009.

Draxler, R. and Hess, G.: An overview of the HYSPLIT 4 modelling system for trajectories, dispersion, and deposition, Aust. Meteorol. Mag., 47, 295–308, 1998.

Frieß, U., Hollwedel, J., Konig-Langlo, G., Wagner, T., and Platt, U.: Dynamics and chemistry of tropospheric bromine explosion events in the Antarctic coastal region, J. Geophys. Res., 109, D06305, doi:10.1029/2003JD004133, 2004.

Herber, A. B., Hass, C., Stone, R. S., Bottenheim, J. W., Liu, P., Li, S.-M., Staebler, R. M., Strapp, J. W., and Dethloff, K.: Regular airborne surveys of Arctic sea ice and atmosphere, Eos Trans. AGU, 93, 41–44, 2012.

Jones, A. E., Anderson, P. S., Wolff, E. W., Roscoe, H. K., Marshall, G. J., Richter, A., Brough, N., and Colwell, S. R.: Vertical structure of Antarctic tropospheric ozone depletion events: characteristics and broader implications, Atmos. Chem. Phys., 10, 7775–7794, doi:10.5194/acp-10-7775-2010, 2010.

Lu, J. Y., Schroeder, W. H., Barrie, L. A., Steffen, A., Welch, H. E., Martin, K., Lockhart, L., Hunt, R. V., Boila, G., and Richter, A.: Magnification of atmospheric mercury deposition to polar regions in springtime: The link to tropospheric ozone depletion chemistry, Geophys. Res. Lett., 28, 3219–3222, doi:10.1029/2000GL012603, 2001.

McConnell, J. C., Henderson, G. S., Barrie, L., Bottenheim, J., Niki, H., Langford, C. H., and Templeton, E. M. J.: Photochemical bromine production implicated in Arctic boundary layer ozone depletion, Nature, 355, 150–152, 1992.

McElroy, C. T., McLinden, C. A., and McConnell, J. C.: Evidence for bromine monoxide in the free troposphere during the Arctic polar sunrise, Nature, 397, 338–341, 1999.

Nakazato, M., Nagai, T., Sakai, T., and Hirose, Y.: Tropospheric ozone differential-absorption lidar using stimulated Raman scattering in carbon dioxide, Appl. Optics, 46, 2269–2279, doi:10.1364/AO.46.002269, 2007.

Oltmans, S.: Surface ozone measurements in clean air, J. Geophys. Res., 86, 1174–1180, 1981.

Oltmans, S. and Komhyr, W.: Surface ozone distributions and variations from 1973–1984 measurements at the NOAA geophysical monitoring for climatic change baseline observatories, J. Geophys. Res., 91, 5229–5236, 1986.

Ridley, B. A., Atlas, E. L., Montzka, D. D., Browell, E. V., Cantrell, C. A., Blake, D. R., Blake, N. J., Cinquini, L., Coffey, M. T., Emmons, L. K., Cohen, R. C., DeYoung, R. J., Dibb, J. E., Eisele, F. L., Flocke, F. M., Fried, A., Grahek, F. E., Grant, W. B., Hair, J. W., Hannigan, J. W., Heikes, B. J., Lefer, B. L., Mauldin, R. L., Moody, J. L., Shetter, R. E., Snow, J. A., Talbot, R. W., Thornton, J. A., Walega, J. G., Weinheimer, A. J., Wert, B. P., and Wimmers, A. J.: Ozone depletion events observed in the high latitude surface layer during the TOPSE aircraft program, J. Geophys. Res., 108, 8356, doi:10.1029/2001JD001507, 2003.

Rothman, L., Gordon, I., and Barbe, A.: The HITRAN 2008 molecular spectroscopic database, J. Quant. Spectrosc. Ra. Transfer, 110, 533–572, doi:10.1016/j.jqsrt.2009.02.013, 2009.

Seabrook, J. A., Whiteway, J., Staebler, R. M., Bottenheim, J. W., Komguem, L., Gray, L. H., Barber, D., and Asplin, M.: LIDAR measurements of Arctic boundary layer ozone depletion events over the frozen Arctic Ocean, J. Geophys. Res., 116, D00S02, doi:10.1029/2011JD016335, 2011.

Steffen, A., Douglas, T., Amyot, M., Ariya, P., Aspmo, K., Berg, T., Bottenheim, J., Brooks, S., Cobbett, F., Dastoor, A., Dommergue, A., Ebinghaus, R., Ferrari, C., Gardfeldt, K., Goodsite, M. E., Lean, D., Poulain, A. J., Scherz, C., Skov, H., Sommar, J., and Temme, C.: A synthesis of atmospheric mercury depletion event chemistry in the atmosphere and snow, Atmos. Chem. Phys., 8, 1445–1482, doi:10.5194/acp-8-1445-2008, 2008.

Full Screen / Esc

Printer-friendly Version

Interactive Discussion
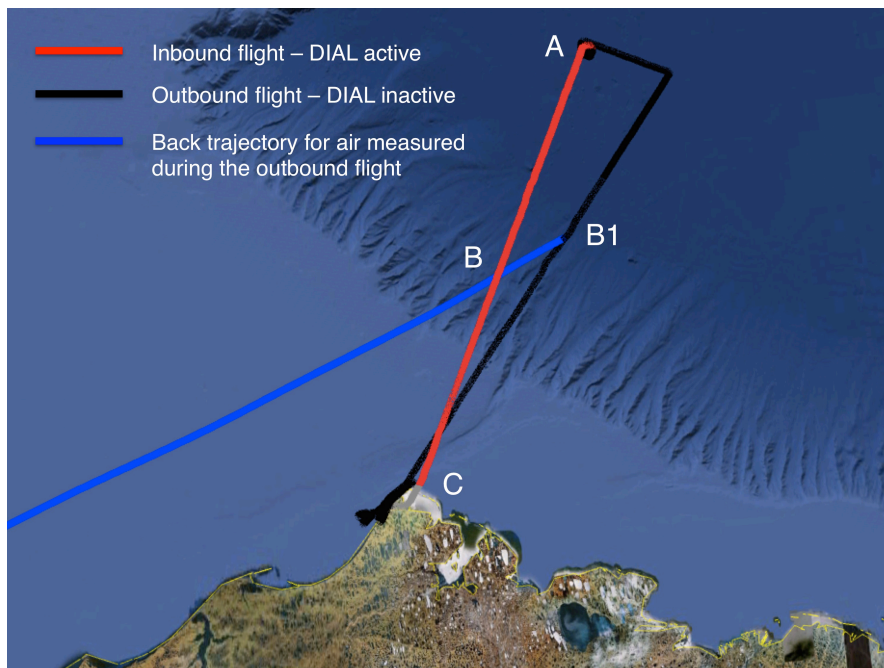
Fig. 1. Ozone DIAL schematic.

Fig. 2. Flight track of the POLAR 5, out of Barrow Alaska. Red indicates the portion of the inbound flight when the ozone DIAL was operational, black the outbound flight. The positions used for the case studies in the analysis are also indicated.

Fig. 3. DIAL measurements of ozone from the ground to 1700 m measured 3 April 2011.
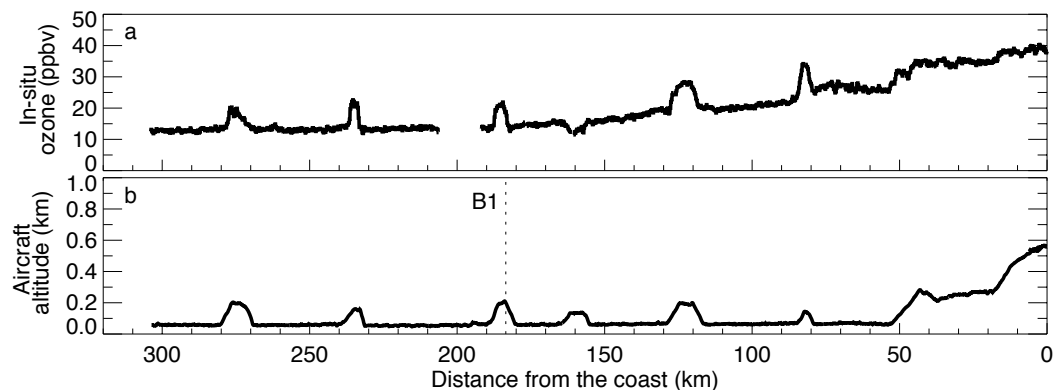
Fig. 4. (a) In-situ ozone measurements along the outbound flight track over the sea ice with the distance from the coast of Alaska (black trace in Fig. 2). **(b)** Aircraft altitude along the outbound flight track.
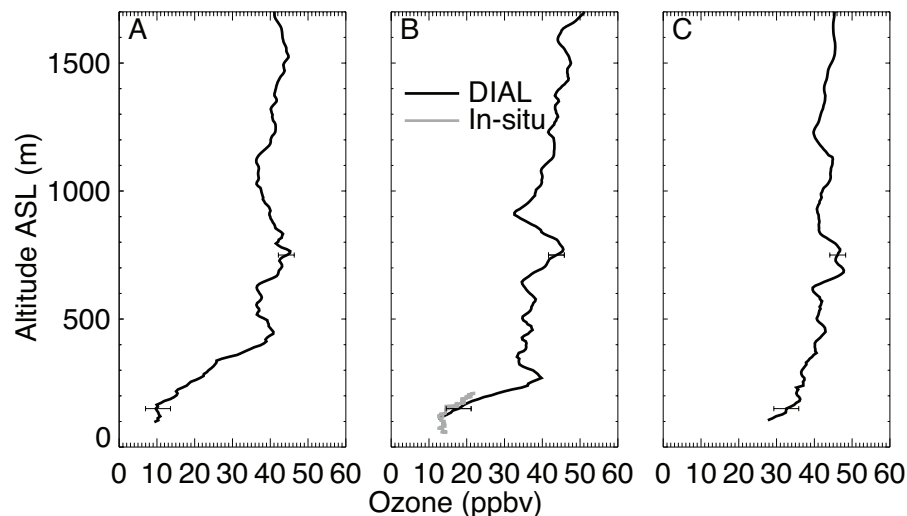
Fig. 5. Measured profiles of ozone mixing ratio with the DIAL along the inbound flight track, and in situ measurements along the outbound flight track (position B1 in Figs. 2 and 4b). Cases **(A)**, **(B)**, and **(C)** correspond to the positions indicated in Figs. 2 and 3. The indicated uncertainty is one standard deviation in the photon counts, propagated through the ozone derivation.
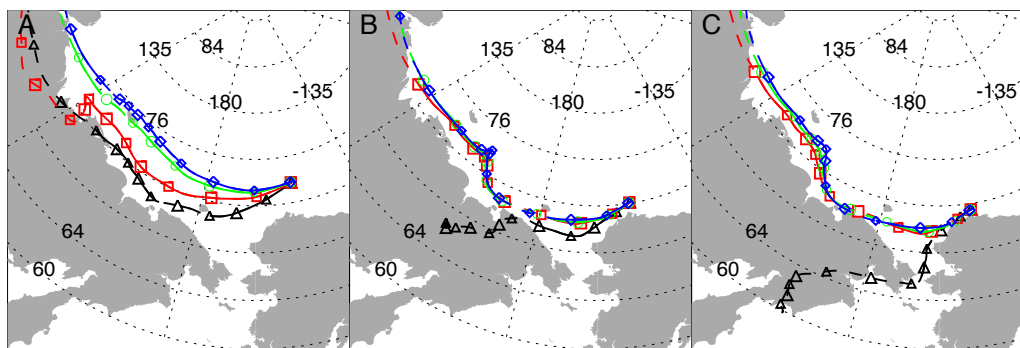
Fig. 6. HYSPLIT back-trajectories of air in which ozone was measured during the April 3rd flight. **(A–C)** correspond to the positions labeled in Figs. 2 and 3. Symbols indicate a period of 12 h has elapsed for the corresponding colored back trajectory.
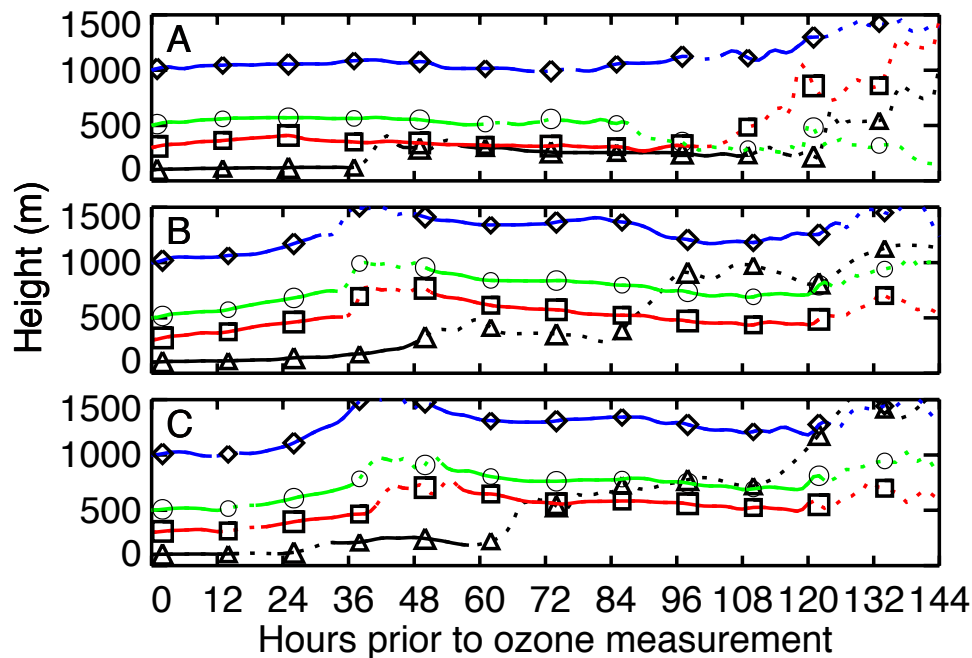
Fig. 7. Altitude history of the calculated back trajectories. **(A–C)** correspond to the times indicated in Fig. 3. Solid lines indicate that the air is over ice, dotted lines indicate land.
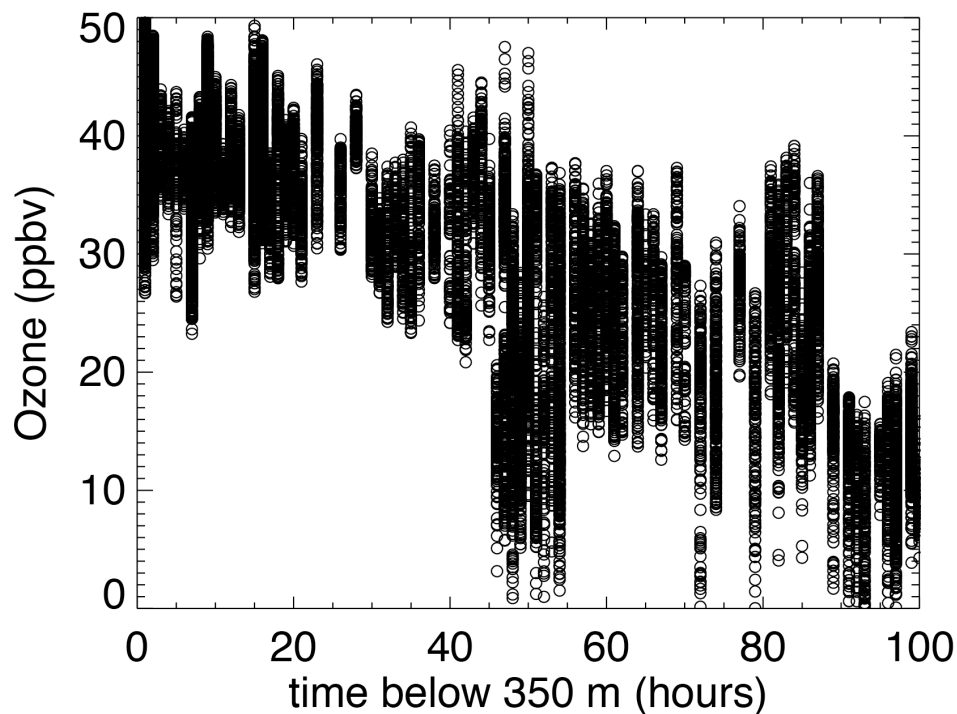
Fig. 8. Measured ozone concentrations vs. time the measured air spent at an altitude of 350 m and lower over the sea ice during the six days prior to being measured.